Adsorption Separation of CH_4/CO_2 on Mesocarbon Microbeads: Experiment and Modeling

Xuan Peng and Wenchuan Wang
Div. of Molecular and Materials Simulation, Key Lab for Nanomaterials, Ministry of Education, Beijing Univ. of Chemical Technology, Beijing 100029, PR China

Ruisheng Xue and Zengmin Shen
National Carbon Fiber Center, College of Materials Engineering, Beijing Univ. of Chemical Technology, Beijing 100029, PR China

DOI 10.1002/aic.10723

A novel meso-porous material, the activated mesocarbon microbeads (a-MCMBs) prepared by this group, is used for the separation of the CH_4/CO_2 mixture by experiment and modeling. First, the adsorption isotherm of nitrogen at 77K was measured to characterize the a-MCMBs by the IGA-003 gravimetric analyzer. Then, the adsorption experiments of pure CH_4 and CO_2 at ambient temperature of 298.15 K were carried out. A CH_4/CO_2 mixture is prepared at the mole ratio of 85:15, corresponding to the gas composition of the Ya-13 gas field in the Qiongdongnan basin, China. Although only the total adsorption amount of the gas mixture on a-MCMBs is available, the single adsorption amount for CH_4 and CO_2, also including the selectivity of CO_2 over CH_4, can be obtained by the Zhou, Gasem, and Robinson Equation of State (ZGR EOS). Finally, the adsorption behavior over a wide range of variables was predicted by the ZGR EOS method. The predicted greatest selectivity of CO_2 over CH_4 is 3.70 at 3.0 MPa, 258.15 K for the feed gas mole composition of CH_4:CO_2 = 40:60. Our results demonstrate that a-MCMBs is not only suitable for CH_4 storage, but also a promising adsorbent for separation of CH_4/CO_2. © 2005 American Institute of Chemical Engineers *AIChE J,* 52: 994–1003, 2006

Keywords: adsorption, activated mesocarbon microbeads, separation, methane, carbon dioxide, EOS

Introduction

Natural gas is mainly composed of methane, carbon dioxide, nitrogen, and heavier hydrocarbons. Because the existence of carbon dioxide reduces the conversion rate and energy content of natural gas,[1,2] there is an increasing need for carbon dioxide separation from natural gas in many industrial fields. Furthermore, in the presence of water, carbon dioxide will corrupt the transportation and storage system.[3] Consequently, some approaches, such as chemical reactive separation, membrane separation, and adsorption,[2] have been developed to remove carbon dioxide. Of these approaches, adsorption is a prospective one for its inherent simplicity, ease of control, low cost, and high energy efficiency.

To develop an adsorption separation technology, researches on the adsorption mechanism are necessary in both theory and experiment. Many researchers have achieved great successes in describing adsorption behavior by different methods, for example, molecular simulation,[4-6] density functional theory (DFT),[7-10] and adsorption models.[11-15] However, adsorption

---

Correspondence concerning this article should be addressed to W. Wang at wangwc@mail.buct.edu.cn.

modeling is still a suitable approach to meet the need for practical applications.

Many theoretical models have been developed for the description of adsorption data for pure components and mixtures, such as the Langmuir model,[16] vacancy solution theory,[17-19] statistical model,[20] ideal adsorbed solution theory,[21,22] heterogeneous ideal adsorbed solution theory, and two-dimensional equations of state (2-D EOS). Among them, Freundlich[23] first presented a model to describe adsorption properties of heterogeneous systems. Later, a theory was developed by Langmuir[24] to describe monolayer adsorption on homogeneous surfaces. Although considerable information is available on single-component adsorption, more concerns are paid to multi-component adsorption processes. A model for multi-component adsorption was first developed by Markham,[25] which is based on the same assumptions as the Langmuir theory for pure gases. Then, the ideal adsorbed solution theory (IAST)[21] was developed for the ideal liquid solution systems[26] as well as non-ideal mixtures,[27,28] where the single-component equilibrium data are only required for the prediction of mixture adsorption. However, due to the assumption of an ideal adsorbed phase, it is not appropriate to predict non-ideal adsorption behavior at high concentrations of adsorbed species with IAST.

As yet, several 2-D EOS models have been applied to gas adsorption, for instance, the VDW,[29,30] virial,[31] and Eyring EOSs.[32] Even so, adsorption models for the prediction of adsorption of mixtures from the adsorption isotherms of pure components seem scarce. In 1994, Zhou, Gasem, and Robinson[33] (ZGR) presented a general 2-D EOS and derived the fugacity expression of the adsorbed phase. They found that the ZGR model can be used to fit pure adsorption isotherms more accurately than the Langmuir model. With the mixing rules, the ZGR EOS can be further used to predict adsorption of gas mixtures. Recently, they made a detailed experimental study for the adsorption of pure N_2, CH_4, CO_2, and their binary mixtures on dry activated carbon, and correlated the experimental data with their model.[34] Their results indicate that ZGR EOS is applicable to the prediction of adsorption behavior for systems containing the major components in natural gas, in particular.

It is well known that an excellent adsorbent is key to adsorption storage of CH_4 and adsorption separation of the CH_4/CO_2 system. As a new type of carbonaceous materials, mesocarbon microbeads (MCMBs) have gradually been used as fillers in paints and as electrical materials.[35,36] The ideal structure of MCMBs is almost like a sphere split by many approximately parallel lamellas.[37] The two adjacent lamellas are treated as a slit-like pore. After an activated treatment by heating the raw carbon spheres and KOH with nitrogen in a furnace, cleaning and drying from the residue of the mixture of petroleum and carbon black, activated mesocarbon microbeads (a-MCMBs) of ellipse shapes sized from 10 to 20 μm have been prepared by our group.[38,39] Scanning electron microscopy (SEM) images[40] taken by a Cambridge S-250 MK III instrument indicate that a single bead of the a-MCMBs exhibits external pores channels, where the fluid molecules can pass through, as shown in Figures 1a and 1b.

It is noticed that CH_4 storage on a-MCMBs was investigated by experiment and computer simulation in our previous work.[40] The adsorption amount of CH_4 on a sample of a-MCMBs can reach 36wt% at 298 K and 4 MPa, which is superior to the results in the literature. This fact encourages us to continue our study on a-MCMBs for the adsorption separation of CH_4/CO_2, which is also a significant subject in the natural gas industry.

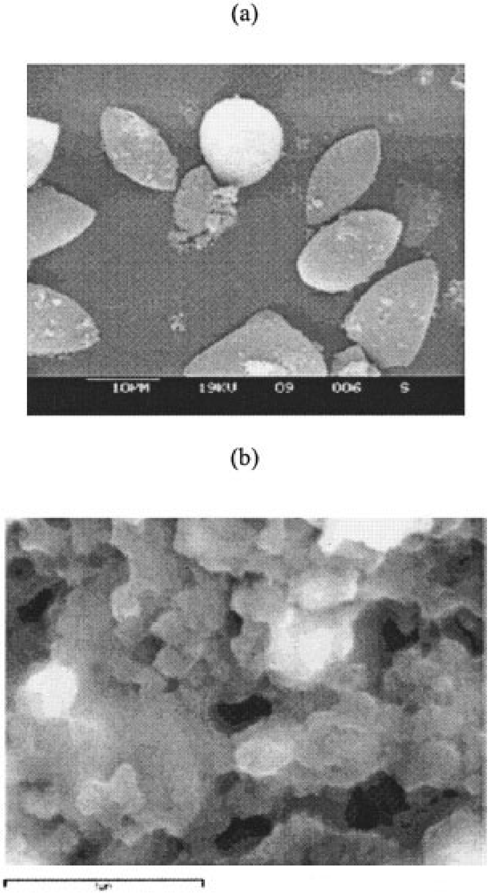

Figure 1. **(a) The SEM photo of a-MCMBs at the voltage of 19 kv, taken from the literature[40]; and (b) The SEM photo of a single bead of a-MCMBs, taken from the literature.[40]**

In this work, a sample of a-MCMBs prepared by our group is used as an adsorbent for the separation of the CH_4/CO_2 mixture. First, the sample is characterized by the adsorption isotherm of nitrogen at 77 K. Then, the adsorption isotherms of pure CH_4, CO_2, and their mixtures are measured with the IGA-003 gravimetric analyzer. Furthermore, the ZGR EOS is used for modeling the separation. Finally, the model proposed is used for the prediction of the selectivities and adsorptive capabilities of the a-MCMBs covering a wide range of compositions of CH_4/CO_2 and pressures at 298.15 K and 258.15 K.

Experimental Studies

IGA-003 instrument

The Intelligent Gravimetric Analyzer (IGA-003, Hiden), a high precision instrument on the basis of gravimetric principles, was used to measure the adsorption isotherms of N_2, CH_4, CO_2, and CH_4/CO_2 mixtures on a-MCMBs. In IGA-003, an ultra-sensitive microbalance of resolution 0.2 μg is mounted in the thermostated heatsink with high precision temperature control. The sample weighed about 100 mg for each run. Before

Table 1. Properties of a-MCMBs, This Work

BET Surface Area	Pore Volume	Average Pore Size[a]
S_{BET}/(m^2 g^{-1})	V_p/(cm^3 g^{-1})	H_{av}/nm
2990	1.9	2.49

[a]Determination of the average pore size can be referred to our previous work.[40]

the measurements, the sample in the vessel of IGA-003 was vacuumed up to 10^{-5} Pa and outgassed at 573 K for about 15 hours. The temperature was set to 77 K by liquid nitrogen and 258.15 K or 298.15 K, respectively, controlled within 0.1% by a built-in water bath. When measuring a data point, a 1.5 hour interim was set to guarantee adsorption equilibration.

Gas samples

Generally, the contents of CH_4 and CO_2 in natural gas vary in a wide range for different geologic structures. For example, the mole fraction of CO_2 for a rich CO_2 natural gas can reach about 0.8,[41] with CH_4 about 0.85[42] for a rich CH_4 natural gas. In our experiment, we prepared our gas mixture from the gas compositions of the Ya-13 natural gas field in the Qiongdongnan basin,[42] one of the largest gas fields in China.[43]

As reported in the literature,[42] the mole fractions of CH_4 and CO_2 fluctuate in the ranges of 83.22 ~ 88.52% and 8.54 ~ 11.50% (mol), respectively, with low concentrations of the components of N_2, C_2, C_3, and C_4, totaling 5-8%. Therefore, only two major components of CH_4 and CO_2 in the natural gas are considered in our work. Pure gases of CH_4 and CO_2 are mixed to resemble a natural gas with a mole ratio of CH_4:CO_2 = 85:15. In addition, the gas sample purities of N_2, CH_4, and CO_2 in our experiments are 99.999%, 99.9%, and 99.995% (mol), respectively, which were all produced by Haipubeifen Gas Industrial Company, Beijing, China.

Characterization of a-MCMBs

It is noted that the sample of a-MCMBs in this work was prepared in a different batch from that in our previous work.[40] Therefore, we characterized our sample again in terms of liquid N_2 adsorption with IGA-003.

The properties of the sample measured on the IGA-003 are listed in Table 1. The sample possesses a high BET surface area of 2990 m^2/g, which is a little lower than the 3180 m^2/g of our previous work.[40] This discrepancy results from the preparation conditions, even though the sample of a-MCMBs used is still of a very high BET specific surface area, more than other a-MCMBs reported.[35,36,44,45] It is also noted that the sample is in the catalog of meso-porous material, with average pore size of 2.49 nm.

Modeling of adsorption separation of CO_2/CH_4

ZGR EOS for Adsorption of Pure Components

In this work, the equation of state (EOS) proposed by Zhou, Gasem, and Robinson (ZGR)[33] was used for modeling of adsorption of the systems in this work, even though it has more parameters than the other EOSs. A major advantage of the ZGR EOS is that it is developed for accurate description of the binary gas adsorption of CH_4/CO_2 on dry activated carbon, in particular. The ZGR EOS is expressed as an analog of the popular three-dimensional equations of state:[33,34]

$$\left[A\pi + \frac{\alpha\omega^2}{1 + U\beta\omega + W(\beta\omega)^2}\right](1 - (\beta\omega)^m) = \omega RT \quad (1)$$

where A is the surface area per mass of adsorbent, π is the spreading pressure, ω is the total amount adsorbed per mass adsorbent, α and β are regressed model constants, m is a parameter added for the model's flexibility, R is the gas constant, and T is temperature. The coefficients $U = 0$, $W = 0$, and $m = 1/3$ are recommended by the literature.[34]

ZGR EOS for Adsorption of Mixtures. When the ZGR EOS is applied to a multi-component system, the model parameters of a gas mixture are calculated by the following mixing rules[33,34]:

$$\alpha = \sum_i \sum_j x_i x_j \alpha_{ij} \quad (2)$$

$$\beta = \sum_i \sum_j x_i x_j \beta_{ij} \quad (3)$$

$$\alpha_{ij} = (1 - C_{ij})(\alpha_i + \alpha_j)/2 \quad (4)$$

$$\beta_{ij} = \sqrt{\beta_i \beta_j}\,(1 + D_{ij}) \quad (5)$$

where x_i and x_j are the mole fractions of components i and j in the adsorbed phase, respectively, and C_{ij} and D_{ij} are the dimensionless interaction parameters. Furthermore, the following equation holds[33,34] at the adsorption equilibrium between the adsorbed and bulk phases:

$$Ax_i\pi\phi_i = k_i RT f_i \quad (6)$$

where f_i is the gas fugacity calculated by the Redlich, Kwong, and Soave (RKS) model[46] for its simplicity and accuracy, k_i is the model constant, denoting the slope of the pure component isotherm at the origin, and θ_i is the fugacity coefficient in the adsorbed phase, given by[33,34]:

$$\ln \phi_i = \frac{2\sum_j \beta_{ij}\omega_j - \beta\omega}{(\beta\omega)^{1-m} - \beta\omega} - \frac{1}{m}\ln[1 - (\beta\omega)^m] - \ln Z_a - \frac{2}{RT}\sum_j \alpha_{ij}\omega_j \quad (7)$$

where Z_a is defined as the compressibility factor in the absorbed phase, $Z_a = \pi A/\omega RT$.

Adsorption of a single component determined by the total uptake of a binary mixture

Only the total uptake for the gas mixture with a constant composition can be measured directly by the IGA-003, rather than the adsorption isotherms of the single component of CH_4 or CO_2. Therefore, an approach should be developed here to solve adsorption of a single component of the binary mixture in terms of the ZGR EOS as follows.

(1) Parameters of α_i and β_i in Eqs. 4 and 5, and k_i in Eq. 6

for pure components ($i = 1,2$) are determined by fitting the experimental isotherms for the two pure components.

(2) Initial interaction parameters C_{ij} and D_{ij} in Eqs. 4 and 5 are guessed.

(3) Initial calculated total adsorption amount, ω_c, and compositions x_i ($i = 1,2$) in the adsorbed phase are guessed.

(4) Parameters of α_{ij} and β_{ij} for the binary mixture are calculated from Eqs. 4 and 5. Then, α and β are calculated from Eqs. 2 and 3.

(5) Calculated total uptake ω_c and x_i ($i = 1,2$) are obtained by solving the nonlinear equations composed of Eq. 6.

(6) A new set of C_{ij}, D_{ij}, ω_c, and x_i ($i = 1,2$) are obtained by minimizing the following objective function F_{obj}, Eq. 8.[33] Otherwise, repeat steps 2 to 6.

$$F_{obj} = \sum_{i=1}^{N_p} \left(\frac{\omega_c(i) - \omega_e(i)}{\omega_e(i)} \right)^2 \tag{8}$$

where N_p is the number of experimental points, and ω_c and ω_e are the calculated and experimental uptakes for pure component i or gas mixture per mass adsorbent, respectively.

In summary, by using the approach proposed above, the adsorption amount of a single component can be solved from the total uptake of a binary mixture, where only the experimental data are available for the CH_4/CO_2 mixture in this work.

To check our approach mentioned above, we calculated the binary gas adsorption of CH_4 and CO_2 studied previously in the literature.[34] Only their experimental total uptakes for the binary mixtures were used to calculate the adsorption amounts of a single component and compared with their experimental ones. The calculated adsorption isotherms of the two single components from the mixture are shown in Figure 2.

Obviously, Figure 2 demonstrates that our calculated uptakes for a single component are in good agreement with the experimental data from the literature,[34] indicating that our approach mentioned above is feasible and reliable for further applications.

Results and Discussion

Adsorption isotherms for pure CH_4 and CO_2 on a-MCMBs

The adsorption isotherms of the pure CH_4 and CO_2 were measured in a pressure range from vacuum up to 1.8 MPa and at 298.15 K by the IGA-003. Note that the pressure is limited to less than 2.0 MPa for the IGA-003 performances. Experimental data of adsorption amounts for pure CH_4 and CO_2 are listed in Tables 2 and 3.

Figure 3 presents the experimental and fitting results for the adsorption isotherms of pure CH_4 and CO_2 on a-MCMBs at 298.15 K. The experimental data show that the adsorption amounts of both the CH_4 and CO_2 increase almost linearly with pressure. Furthermore, when the pressure increases up to 1.8 MPa, the adsorption amount of CH_4 reaches about 13.54wt%, which is about one fifth of CO_2, 78.70wt%. The regressed model parameters for the pure components are listed in Table 4.

From Figure 3 and Table 4, it is found that the calculated adsorption amounts are in good agreement with the experimental data for the pure CH_4 and CO_2, though the ARD for CO_2 is about 5.59%, being a little larger than that of 3.04% for CH_4, where ARD, the average relative percent deviation, is defined as:

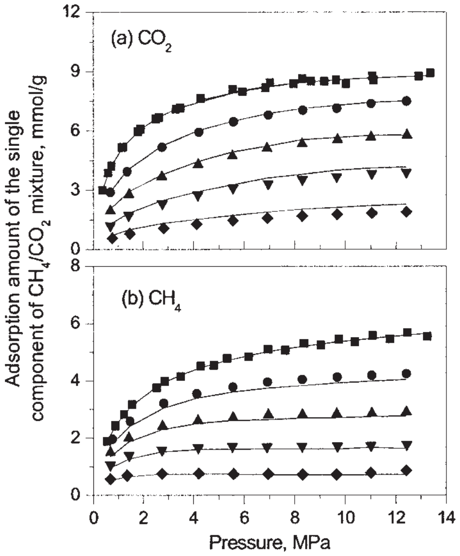

Figure 2. Comparison of the calculated adsorption amount of a single component from the total experimental uptake of CH_4/CO_2 mixture with experimental data on dry activated carbon at 318.2 K in the literature,[34] — calculated, this work, ■ 100%(mol), ●80.0%, ▲ 60.0%, ▼ 40.0%, ◆ 20.0%.

(a) CO_2, (b) CH_4.

$$\mathrm{ARD} = \frac{100}{N_p} \sum_{i=1}^{N_p} \left| \frac{\omega_c(i) - \omega_e(i)}{\omega_e(i)} \right| \tag{9}$$

Adsorption isotherm for CH_4/CO_2 mixture

To investigate the adsorptive separation capability of a-MCMBs for the CH_4/CO_2 mixture, the adsorption amounts of the feed mixture $CH_4:CO_2 = 85:15$ were measured on a-MCMBs at 298.15 K, and are listed in Table 5. The isotherm of the total adsorption is shown in Figure 4. The highest pressure range is also less than 2.0 MPa due to the limit of IGA-003.

As shown in Figure 4, the total amount increases linearly with the pressure, which is similar to the adsorption isotherm of pure CH_4 and CO_2. In addition, the total adsorption amount rises up to 21.7wt% at 1.8 MPa for the existence of CO_2 on the a-MCMBs.

Figure 4 presents the calculated adsorption by using the ZGR EOS for mixtures. Meanwhile, parameters C_{ij} and D_{ij} in Eqs. 4 and 5 are obtained by fitting to the experimental data. It is seen from Figure 4 that the calculated and experimental total uptakes coincide well with ARD about 5.47% for 25 experimental data points. As pointed out in the literature,[33] if C_{ij} and D_{ij} are set to zero, the EOS is termed as "predictive mode," while it is termed as "correlative mode" for adoption of nonzero interaction parameters. In fact, the regressed parameters C_{ij} and D_{ij} here are of insignificant values of 1.17E-06 and 6.67E-07,

Table 2. Experimental Data for Pure CH_4 Adsorption on a-MCMBs at 298.15 K, Measured by IGA-003 Gravimetric Analyzer

Pressure (MPa)	Adsorption (wt%)	Adsorption (mmol/g)	Pressure (MPa)	Adsorption (wt%)	Adsorption (mmol/g)
0.0198	0.763	0.4757	0.5000	6.234	3.8855
0.0248	0.847	0.5277	0.5999	7.060	4.4009
0.0498	1.236	0.7703	0.6998	7.816	4.8721
0.0748	1.606	1.001	0.7997	8.524	5.3132
0.1000	1.970	1.2281	0.8997	9.171	5.7164
0.1249	2.311	1.4407	0.9998	9.781	6.0967
0.1499	2.637	1.6437	1.0996	10.354	6.4538
0.1749	2.948	1.8376	1.1997	10.902	6.7953
0.1997	3.251	2.0266	1.3997	11.865	7.3956
0.2997	4.353	2.7133	1.5998	12.748	7.9462
0.4000	5.342	3.3296	1.7996	13.538	8.4387

respectively. C_{ij} and D_{ij} are, therefore, both set to zero, and the "predictive mode" is adopted directly for further predictions in this work.

Predictions of adsorption for CH_4/CO_2 mixtures on a-MCMBs

To evaluate adsorptive and separation capabilities of a-MCMBs, extensive predictions were carried out by using the model proposed here, covering a wide range of variables.

Pressure Range and Temperatures in Predictions. If the pressure is chosen too high in our predictions, condensation would occur in the bulk gas phase, which is not suitable for the calculation of the gas fugacity coefficient in Eq. 6. Thus, it is necessary to determine the dew-point temperatures of the bulk CH_4/CO_2 mixtures at different gas compositions. The dew-point calculations for the bulk CH_4/CO_2 mixtures by the Peng-Robinson EOS[47] were carried out here. A phase diagram was prepared, which is not shown in the text for brevity, to ensure that all the predictions should be performed at the temperature and pressure where no condensation occurs in the bulk phase.

The ambient temperature of 298.15 K is chosen for its availability in industrial applications. In addition, in view of current refrigeration technology widely applied in industry, another temperature is set to 258.15 K in the present work.

Compositions in predictions. To cover a wide range of the natural gas compositions, five feed mole ratios for the CH_4/CO_2 mixtures, which are 20:80, 40:60, 60:40, 80:20 and 85:15, were calculated by using the model proposed here. Figure 5 shows the calculated fractional and total uptakes for the mixtures at 298.15 K and 258.15 K, respectively.

It is noticed that in Figures 5(a-5) and 5(b-5) the pressures predicted are limited to not beyond 3.4 MPa and 1.4 MPa, respectively, because in these cases the mole fractions of CO_2 in the adsorbed phases are about 1.0 at 298.15 K and 258.15 K. In addition, as shown in Figure 5(b-4), the pressures predicted are below 4.0 MPa to avoid condensation in the bulk gas mixtures at 258.15 K.

It is found from Figure 5 that the adsorption amounts for the single component of CH_4 and CO_2 and their binary mixture all increase with pressure at 298.15 K and 258.15 K. It is also found that at the high mole fraction of CH_4 (0.85) in the feed gas mixture, the fractional uptake of CH_4 is only slightly higher than that of CO_2 (see Figures 5(a-1) and 5(b-1)). Furthermore, the adsorption amount of CH_4 decreases with the increase of the mole fraction of CO_2 in the feed gas from 0.15 to 0.8. Different from Figure 5a, Figure 5b shows that at the lower temperature of 258.15 K, the uptakes of CO_2 and the binary mixture are all higher than those at 298.15 K. For example, at 3.0 MPa and the mole fraction of CO_2 in the feed gas of 0.6, the fractional uptake of CO_2 and the total uptake are 57.31wt% and 62.1wt% at 298.15 K, against 71.6wt% and 76.32wt% at 258.15 K, respectively. It indicates that the adsorption of the mixture and CO_2 is favored at low temperatures.

Adsorption selectivities for CH_4/CO_2 mixtures

To investigate the separation capability of CO_2 over CH_4 on a-MCMBs, the selectivity S_{CO_2} is defined by:

Table 3. Experimental Data for Pure CO_2 Adsorption on a-MCMBs at 298.15 K, Measured by IGA-003 Gravimetric Analyzer

Pressure (MPa)	Adsorption (wt%)	Adsorption (mmol/g)	Pressure (MPa)	Adsorption (wt%)	Adsorption (mmol/g)
0.0199	1.988	0.4518	0.6996	42.929	9.7543
0.0248	2.445	0.5556	0.8000	47.208	10.7267
0.0498	4.636	1.0535	0.8999	51.037	11.5966
0.0747	6.696	1.5215	0.9999	54.653	12.4182
0.0997	8.680	1.9722	1.0996	58.155	13.2141
0.1248	10.583	2.4047	1.1998	61.490	13.9718
0.1497	12.405	2.8187	1.2998	64.593	14.6769
0.1747	14.185	3.2231	1.4001	67.571	15.3536
0.1998	15.907	3.6145	1.4999	70.509	16.0211
0.2997	22.373	5.0836	1.5997	73.292	16.6535
0.3997	28.204	6.4085	1.6997	76.043	17.2785
0.4997	33.518	7.6159	1.7997	78.703	17.8829
0.5996	38.438	8.734			

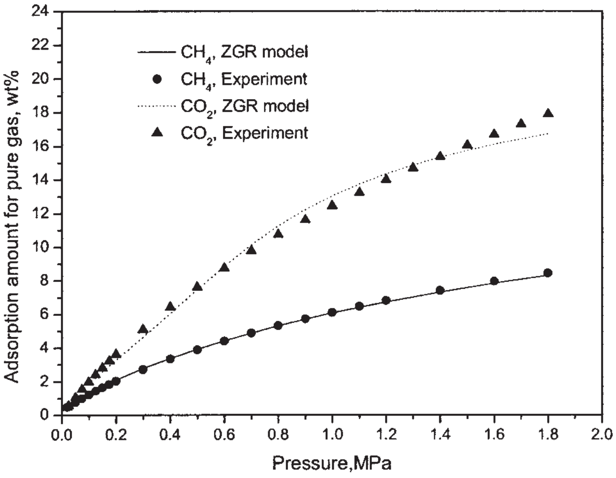

Figure 3. Calculated and experimental results for the adsorption of pure CH_4 and CO_2 on a-MCMBs at 298.15 K.

$$S_{CO_2} = \frac{x_{CO_2}/x_{CH_4}}{y_{CO_2}/y_{CH_4}} \tag{10}$$

where x_{CO_2} and y_{CO_2} are the mole fractions of CO_2 in the adsorbed phase and bulk gas phase, respectively.

Figure 6 presents the change of S_{CO_2} with pressure at different gas compositions, 298.15 K and 258.15 K, respectively. It is found from Figure 6a that S_{CO_2} increases with pressure first and flattens out at high pressures. In contrast, Figure 6b demonstrates that S_{CO_2} increases with pressure first, then after reaching their highest points, declines moderately. Table 6 gives the maximum values of S_{CO_2} and their pressures at different mole fractions of CO_2 in the feed gases and 258.15 K. It is found that for the gas composition of CH_4:CO_2 = 40:60, the greatest S_{CO_2} of 3.70 is obtained at 3.0 MPa and 258.15 K.

Figure 7 shows S_{CO_2} changing with the composition of CO_2 in the feed gas at 1.0, 3.0, and 5.0 MPa and 298.15 K and 258.15 K, respectively. In general, higher pressures exhibit greater values of S_{CO_2} over the composition range of interest. Interestingly, the values of S_{CO_2} are almost the same for $P =$ 3.0 and 5.0 MPa at 258.15 K, while a slight difference appears at 298.15 K. Consequently, a favorable operation pressure of 3.0 MPa is recommended. To investigate the effect of temperature on selectivity, S_{CO_2} is plotted against CO_2 composition at $P =$ 1.0, 3.0 and 5.0 MPa in Figure 8. As is seen, higher values of S_{CO_2} are attained at the lower temperature of 258.15 K, and a pronounced increase of S_{CO_2} with CO_2 composition occurs at 3.0 MPa in particular.

Table 4. Calculated Results and Regressed ZGR EOS Parameters for Adsorption of Pure CH_4 and CO_2 on a-MCMBs at 298.15 K

	Parameters				
Component	α	β	ln k	N_p[a]	ARD[b]
CH_4	3945.370	0.03372	1.68715	22	3.04
CO_2	4101.871	0.02659	1.96461	25	5.59

[a] N_p is number of data points evaluated.
[b] Definition of ARD is given by Eq. 9.

Table 5. Experimental Results for the Gas Mixture of CH_4/CO_2 Adsorption on a-MCMBs at 298.15 K and Mole Ratio of CH_4:CO_2 = 85:15, Measured by IGA-003 Gravimetric Analyzer

Pressure (MPa)	Adsorption (wt%)	Pressure (MPa)	Adsorption (wt%)
0.0200	0.803	0.7000	12.278
0.0249	0.904	0.7998	13.421
0.0499	1.504	0.9000	14.486
0.0748	2.128	1.0000	15.495
0.0999	2.698	1.0998	16.430
0.1249	3.259	1.1998	17.312
0.1499	3.791	1.2997	18.129
0.1749	4.296	1.3999	18.916
0.2000	4.791	1.5000	19.671
0.2998	6.599	1.5998	20.371
0.4000	8.223	1.7001	21.078
0.5001	9.681	1.7997	21.698
0.5998	11.021		

Conclusions

Adsorption storage and purification of natural gas is an important and challenging subject in front of chemical engineers. A novel adsorbent, the activated mesocarbon microbeads (a-MCMBs) prepared by our group, has been used for storage of methane, the major component of natural gas, and hydrogen with good results.[40] In addition to the storage of methane, we focus on the separation capability of the a-MCMBs for removal of the major impurity CO_2 by adsorption in this work.

To characterize our sample, the adsorption isotherm of N_2 on the a-MCMBs was measured at 77 K by a high precision instrument, the IGA-003 gravimetric analyzer. The results indicate that the a-MCMBs are a meso-porous material with the high BET specific area of 2990 m^2/g and average pore size 2.49 nm, as shown in Table 1.

Experimental isotherms on the a-MCMBs for pure CH_4, CO_2, and a CH_4/CO_2 mixture at the mole ratio of 85:15, corresponding to the gas composition of the Ya-13 gas field in the Qiongdongnan basin of China,[42] were measured by the IGA-003 at 298.15 K and from vacuum up to about 2.0 MPa. As seen in Figure 3, the a-MCMBs exhibit excellent adsorptive capacity, with uptakes 13.54wt% for CH_4 and 78.70wt% for

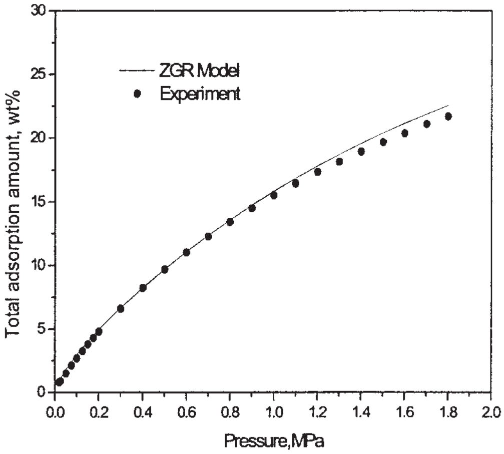

Figure 4. Total adsorption amount (wt%) of CH_4/CO_2 mixture on a-MCMBs at 298.15 K by Experiment and ZGR Model.

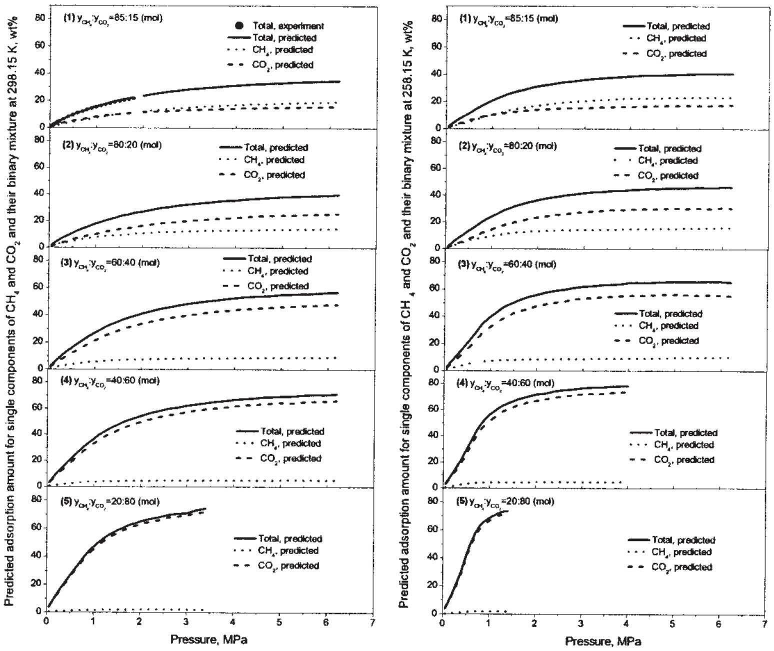

(a) T=298.15K (b) T=258.15K

Figure 5. Predicted adsorption amount for single components of CH_4 and CO_2 and their binary mixture at (a) T = 298.15 K and (b) T = 258.15 K.

(1) Gas composition of CH_4:CO_2 = 85:15 (mol); (2) gas composition of CH4:CO2 = 80:20; (3) gas composition of CH_4:CO_2 = 60:40; (4) gas composition of CH_4:CO_2 = 40:60; (5) gas composition of CH_4:CO_2 = 20:80.

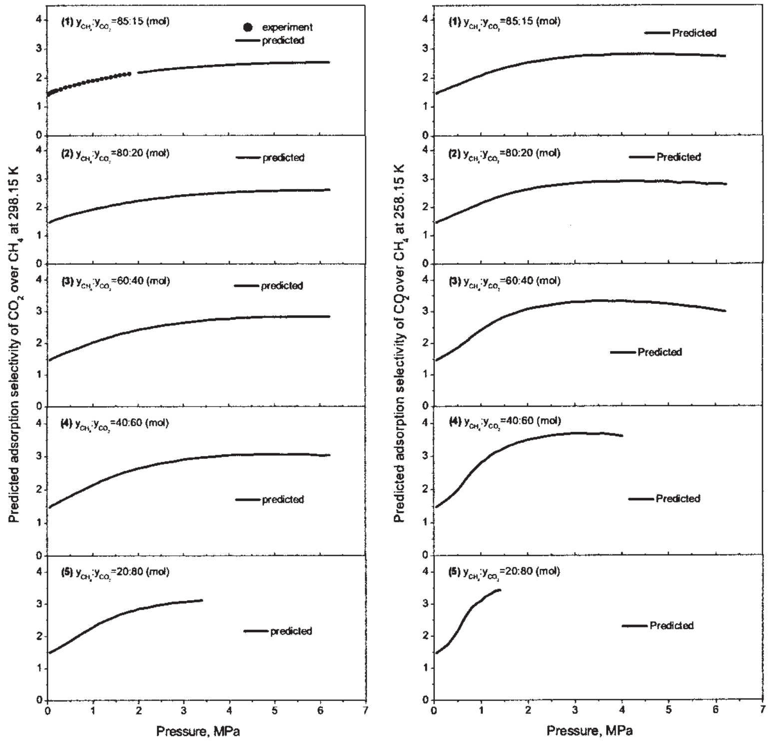

(a) T=298.15K (b) T=258.15K

Figure 6. Predicted adsorption selectivity of CO_2 over CH_4 at (a) T = 298.15 K and (b) T = 258.15 K.

(1) Gas composition of CH_4:CO_2 = 85:15 (mol); (2) gas composition of CH_4:CO_2 = 80:20; (3) gas composition of CH_4:CO_2 = 60:40; (4) gas composition of CH_4:CO_2 = 40:60; (5) gas composition of CH_4:CO_2 = 20:80.

Table 6. Maximum Values of S_{CO_2} and Corresponding Pressures at Different Mole Fractions of CO_2 in Feed Gas Mixtures and 258.15 K

	Mole Fraction of CO_2 in Feed Gas Mixture				
	0.15	0.2	0.4	0.6	0.8
$S_{CO_2,max}$	2.82	2.92	3.33	3.70	3.43
P (MPa)	4.2	4.4	3.4	3.0	1.4

CO_2 at 1.8 MPa, respectively (see detailed data in Tables 2 and 3).

To evaluate the separation capability of a-MCMBs extensively, modeling of the selective adsorption is essential. We introduce the Zhou, Gasem, and Robinson Equation of State (ZGR EOS)[33] for the description of pure and mixture adsorption due to its accuracy for CH_4 and CO_2 systems, in particular. The calculated results are in good agreement with the experimental data for both the pure components and the mixture, as shown in Figures 3 and 4. It is noticed that the IGA-003 can measure only the total adsorption of a mixture directly. Therefore, an approach is developed here to calculate the adsorption for a single component of the mixture from the total uptake at a constant feed gas composition and temperature. The method has been rigorously tested by experimental data in the literature[34] with good accuracy, as seen in Figure 2. Consequently, the adsorption separation of CH_4/CO_2 mixtures can be satisfactorily modeled by the approach proposed in this work.

The adsorption selectivity of CO_2 over CH_4, S_{CO_2}, was extensively calculated on the ZGR EOS and the method proposed in this work, covering wide ranges of compositions and pressures at ambient temperature T = 298.15 and a commonly used refrigeration temperature T = 258.15 K. It is found that S_{CO_2} increases monotonically with pressure at 298.15 K for five different compositions of the feed mixtures from y_{CH_4} = 0.20 = 0.20 to 0.85. However, the increase of pressure would not enhance the selectivity pronouncedly at the high y_{CH_4} values. Greater selectivities are attained at the low temperature of 258.15 K, compared with those at 298.15 K. In addition, the selectivities are almost unchanged at 258.15 K, and exhibit only a slight increase when the pressure increases from 3.0 to 5.0 MPa at 298.15 K. It is found that the predicted greatest selectivity of CO_2 over CH_4 is 3.70 at 3.0 MPa, 258.15 K for the feed gas mole composition of CH_4:CO_2 = 40:60.

In conclusion, our experimental and calculated results indicate that a-MCMBs are not only an excellent adsorbent for storage of methane, as reported in our previous work,[40] but also a prospective material for removal of CO_2, the major impurity in natural gases. Furthermore, the approach recommended in this work can be used for the determination of separation conditions in adsorptive separations, concerning different natural gas compositions. It should be pointed out that the compositions of natural gases are rather complicated for containing not only CH_4 and CO_2, but also some impurities, such as nitrogen and C_2-C_4 hydrocarbons. The contents of the impurities vary from 5-8% (mol), as reported in the literature.[42] The impurities will certainly influence the separation of the CH_4/CO_2 system on a-MCMBs. Furthermore, particulate a-MCMBs should be processed by granulation for an industrial adsorbent. These are topics to be addressed in our future work.

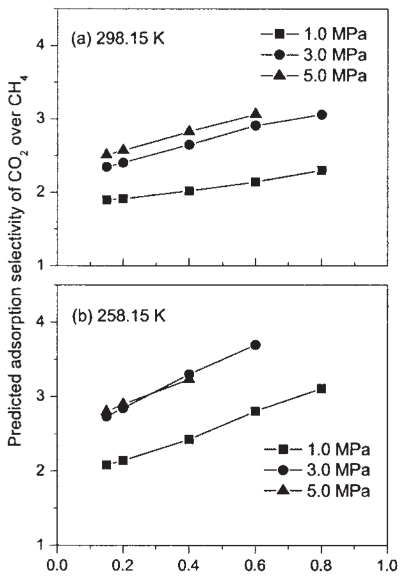

Figure 7. Predicted adsorption selectivity of CO_2 over CH_4.

—■—, 1.0 MPa; —●—, 3.0 MPa; —▲—, 5.0 MPa. (a) 298.15 K, (b) 258.15 K.

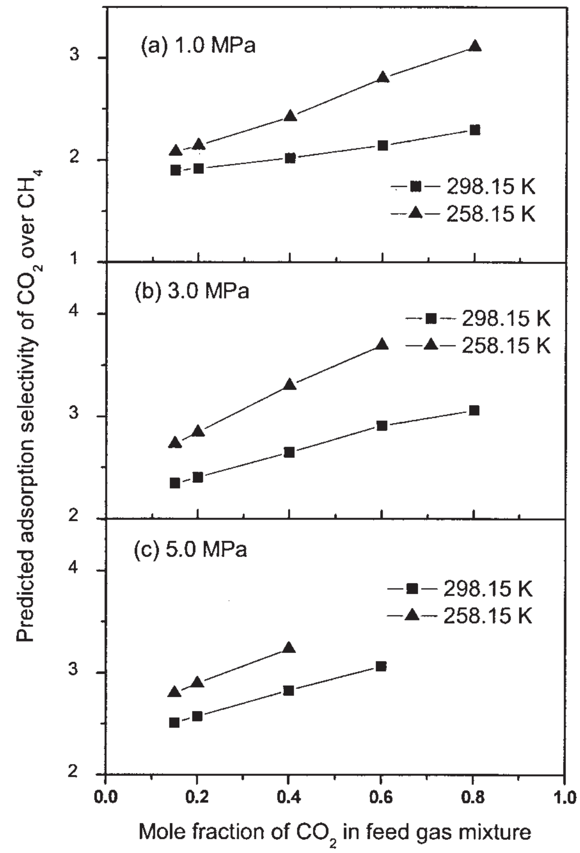

Figure 8. Predicted adsorption selectivity of CO_2 over CH_4.

—■—, 298.15 K; —▲—, 258.15 K. (a) 1.0 MPa, (b) 3.0 MPa, (c) 5.0 MPa.

Acknowledgments

This work was supported by the National Basic Research Program (No. 203CB615807), and the National Natural Science Foundation of China (No. 20236010).

Notation

A = surface area per mass of adsorbent, $10^{-4} \cdot m^2/kg$
π = spreading pressure, $10^3 \cdot Pa \cdot m$
ω = the total amount adsorbed per mass adsorbent, mol/kg
α = regressed model constants calculated by Eq. 2 ($10^{-1} \cdot Pa \cdot m^3 \cdot kg)/(mol \cdot mol)$
β = regressed model constants calculated by Eq. 3, kg/mol
m = model parameter, dimensionless
R = universal gas constant, $10^{-1} \cdot Pa \cdot m^3/(mol \cdot K)$
T = absolute temperature, K
U, W = model coefficients, dimensionless
x_i, x_j = mole fraction of component i and j in adsorbed phase, respectively, dimensionless
α_i, α_j = regressed model constants of component i and j, respectively, $(10^{-1} \cdot Pa \cdot m^3 \cdot kg)/(mol \cdot mol)$
β_i, β_j = regressed model constants of component i and j, respectively, kg/mol
α_{ij}, β_{ij} = interaction model constants calculated by Eqs. 4 and 5, respectively
C_{ij} = interaction parameter, dimensionless
D_{ij} = interaction parameter, dimensionless
θi = fugacity coefficient of component i in adsorbed phase, dimensionless
k_i = model constant of pure component i, $10^{-5} \cdot mol/(Pa \cdot kg)$
f_i = fugacity of component i in gas bulk phase, $10^3 \cdot Pa \cdot m$
Z_a = compress factor of adsorbed phase
F_{obj} = objective function, dimensionless
ω_c = the calculated uptakes for pure component i or gas mixture per mass adsorbent, mol/kg
ω_e = the experimental uptakes for pure component i or gas mixture per mass adsorbent, mol/kg
N_p = number of data points evaluated
ARD = average relative percent deviation, dimensionless
S_{CO_2} = adsorption selectivity of CO_2 over CH_4, dimensionless
x_{CO_2}, y_{CO_2} = mole fractions of CO_2 in adsorbed and bulk gas phase, respectively, dimensionless
x_{CH_4}, $y_{CH}4$ = mole fractions of CH_4 in adsorbed and bulk gas phase, respectively, dimensionless

Literature Cited

1. Hernández-Maldonado AJ, Yang RT, Chinn D, Munson CL. Partially calcined gismondine type silicoaluminophosphate SAPO-43: isopropylamine elimination and separation of carbon dioxide, hydrogen sulfide, and water. *Langmuir*. 2003;19:2193-2200.
2. Sarkar SC, Bose A. Role of activated carbon pellets in carbon dioxide removal. *Energy Conversion and Management*. 1997;38:S105-S110.
3. Li SG, Falconer JL, Noble RD. SAPO-34 membranes for CO_2/CH_4 separation. *Journal of Membrane Science*. 2004;241:121-135.
4. Jiang JW, Sandler SI. Nitrogen and oxygen mixture adsorption on carbon nanotube bundles from molecular simulation. *Langmuir*. 2004; 20:10910-10918.
5. He YF, Seaton NA. Experimental and computer simulation studies of the adsorption of ethane, carbon dioxide, and their binary mixtures in MCM-41. *Langmuir*. 2003;19:10132-10138.
6. Do DD, Do DH. Adsorption of ethylene on graphitized thermal carbon black and in slit pores: a computer simulation study. *Langmuir*. 2004; 20:7103-7116.
7. Libby B, Monson PA. Adsorption/desorption hysteresis in inkbottle pores: a density functional theory and monte carlo simulation study. *Langmuir.* 2004;l20:4289-4294.
8. Yan B, Yang XN. Binary adsorption of benzene and supercritical carbon dioxide on carbon: density functional theory study. *Ind Eng Chem Res*. 2004;43:6577-6586.
9. Sweatman MB, Quirke N. Predicting the adsorption of gas mixtures: adsorbed solution theory versus classical density functional theory. *Langmuir*. 2002;18:10443-10454.
10. Ustinov EA, Do DD. High-pressure adsorption of supercritical gases on activated carbons: an improved approach based on the density functional theory and the bender equation of state. *Langmuir*. 2003; 19:8349-8357.
11. Cavenati S, Grande CA. Adsorption equilibrium of methane, carbon dioxide, and nitrogen on zeolite 13X at high pressures. *J Chem Eng Data*. 2004;49:1095-1101.
12. Yun JH, Tina D, Frerich JK, Nigel AS. Adsorption of methane, ethane, and their binary mixtures on MCM-41: experimental evaluation of methods for the prediction of adsorption equilibrium. *Langmuir*. 2002; 18:2693-2701.
13. Choi BU, Choi DK, Lee YW, Lee BK. Adsorption equilibria of methane, ethane, ethylene, nitrogen, and hydrogen onto activated carbon. *J Chem Eng Data*. 2003;48:603-607.
14. Soule AD, Smith CA, Yang XN, Lira CT. Adsorption modeling with the ESD equation of state. *Langmuir*. 2001;17:2950-2957.
15. Harlick PJE, Tezel FH. Adsorption of carbon dioxide, methane and nitrogen: pure and binary mixture adsorption for ZSM-5 with SiO_2/ $Al2O_3$ ratio of 280. *Separation and Purification Technology*. 2003;33: 199-210.
16. Markham ED, Benton AF. The adsorption of gas mixtures by silica. *J Am Chem Soc*. 1931;53:497-506.
17. Suwanayuen S, Danner RP. A gas adsorption isotherm equation based on vacancy solution theory. *AIChE J*. 1980;26:68-75.
18. Suwanayuen S, Danner RP. Vacancy solution theory of adsorption from gas mixtures. *AIChE J*. 1980;26:76-83.
19. Cochran TW, Knaebel RL, Danner RP. Vacancy solution theory of adsorption using Flory-Huggins activity coefficient equations. *AIChE J*. 1985;31:268-277.
20. Ruthven DM, Wong F. Generalized statistical model for the prediction of binary adsorption equilibria on zeolites. *Ind Eng Chem Fundam*. 1985;24:27-32.
21. Myers AL, Prausnitz JM. Thermodynamics of mixed-gas adsorption. *AIChE J*. 1965;11:121-127.
22. Malek A, Farooq S. Comparison of isotherm models for hydrocarbon adsorption on activated carbon. *AIChE J*. 1996;42:3191-3201.
23. Freundlich HZ. Adsorption in solution. *Phys Chem*. 1906;57:384-470.
24. Langmuir I. The adsorption of gases on plane surface of glass mica and platinum. *J Am Chem Soc*. 1918;40:1361-1402.
25. Do DD. *Adsorption Analysis: Equilibrium and Kinetics*, 1st ed. London: Imperial College Press; 1988.
26. Radke CJ, Prausnitz JM. Thermodynamics of multi-solute adsorption from dilute liquid solutions *AIChE J*. 1972;18:761-768.
27. Talu O, Zwiebel I. Multicomponent adsorption equilibria of nonideal mixtures. *AIChE J*. 1986;32:1263-1276.
28. Lee CS, Belfort G. Thermodynamics of multi-solute adsorption from dilute liquid solution: I. The use of an equation of state. *Ind Eng Chem Res*. 1988;27:951-956.
29. Hill TL. Theory of multimolecular adsorption from a mixture of gases. *J Chem Phys*. 1946;14:268-275.
30. de Boer JH. *The Dynamical Character of Adsorption.* London: Oxford University Press; 1953.
31. Hoory SE, Prausnitz JM. Monolayer adsorption of gas mixtures on homogeneous and heterogeneous solids. *Chem Eng Sci*. 1967;22:1025-1033.
32. DeGance AE. Multicomponent high-pressure adsorption equilibria on carbon substrates: theory and data. *Fluid Phase Equilib*. 1992;78:99-137.
33. Zhou C, Hall F, Gasem AM, Robinson RL. Predicting gas adsorption using two-dimensional equations of state. *Ind Eng Chem Res*. 1994; 33:1280-1289.
34. Sudibandriyo M, Pan Z, Fitzgerald JE, Robinson RL, Gasem AM. Adsorption of methane, nitrogen, carbon dioxide, and their binary mixtures on dry activated carbon at 318.2 K and pressures up to 13.6 MPa. *Langmuir*. 2003;19:5323-5331.
35. Ishii C, Kaneko K. Surface and physical properties of microporous carbon spheres. *Prog Org Coatings*. 1997;31:147-152.
36. Ishii C, Matsumura Y, Kaneko K. Ferromagnetic behavior of superhigh surface-area carbon. *J Phy Chem*. 1995;99:5743-5746.
37. Shao XH, Huang SP, Shen ZG, Chen JF. Adsorption study of methane on activated mesocarbon microbeads by density functional theory. *Chinese Journal of Chemistry*. 2004;22:142-147.
38. Xue RS, Shen ZM. The activation of the mesophase pitch microbeads. *Carbon Technol* (in Chinese). 2001;5:1-5.

39. Xue RS, Shen ZM. Effects of KOH/MMB weight ratio on structure and morphology of activated mesophase carbon microbeads. *Mater Sci Technol* (in Chinese). 2002;10:346-351.
40. Shao XH, Wang WC, Xue RS, Shen ZM. Adsorption of methane and hydrogen on mesocarbon microbeads by experiment and molecular simulation. *J Phys Chem B*. 2004;108:2970-2978.
41. He JX, Liu QW. Analysis and discussion on the generative cause, migration and distribution of CO_2 in Ying-Qiong basins in the north of the south China sea. *Natural Gas Geoscience* (in Chinese). 2004;15: 12-19.
42. Chen DF, Zhao ZH, Xie QL, Xu WX, Yao BC. Prediction of pressure-temperature and thickness below seafloor of gas hydrate formation of natural gases from Ya-13 gas field in Qiongdongnan basin. *Geochimica* (in Chinese). 2001;30:585-591.
43. Wang MF. A comparison of petroleum accumulation between YA13–1 structure and YA21–1 structure in Yanan depression within Qiongdongnan basin. *Acta Geoscientia Sinica* (in Chinese). 2002;23: 559-562.
44. Wang YG, Egashira M, Ishida S, Korai Y, Ochida I. Microstructure of mesocarbon microbeads prepared from synthetic isotropic naphthalene pitch in the presence of carbon black. *Carbon*. 1998;37:307-314.
45. Korai Y, Wang YG, Yoon SH, Ishida S, Mochida I, Nakagawa Y, Matsumura Y. Effects of carbon black addition on preparation of meso-carbon microbeads. *Carbon*. 1997;35:875-884.
46. Soave G. Equilibrium constants from a modified Redlich-Kwong equation of state. *Chem Eng Sci*. 1972;27:1197-1203.
47. Peng DY, Robinson DB. A new two-constant equation of state. *Ind Eng Chem Fundam*. 1976;15:59-64.

Manuscript received Mar. 31, 2005, and revision received Sept. 30, 2005.